JOURNAL OF MATERIALS SCIENCE 8 (1973) 1595–1602

# Dependence of room temperature fracture strength on strain-rate in sapphire

J. T. A. POLLOCK*, G. F. HURLEY
*Tyco Laboratories, Inc, Waltham, Massachusetts, USA*

Single crystal, *c*-axis oriented sapphire filaments have been tension tested as a function of surface conditions and environment, and as a function of strain-rate. Filaments in the as-grown condition were shown to have failure strengths independent of the amount of water in the environment when tested at 0.002 $min^{-1}$. This independence was correlated with fractographic determinations showing internal nucleation of fracture. In contrast, introduction of surface flaws was shown to reduce the strength to a level dependent upon the moisture content of the test environment. Filaments having as-grown surfaces were shown to fail at strength levels dependent upon the strain-rate. When the latter was increased stepwise in order of magnitude from 0.002 to 2.0 $min^{-1}$, the fracture strength increased by a total of $\sim$ 70 kg $mm^{-2}$, or $\sim$ 30% of the lowest average value. It is argued that the latter behaviour is different from static fatigue and that it is consistent with the Orowan model of subcritical crack extension in brittle materials. Experimental data are used to calculate background flaw sizes in the range of 0.22 to 0.39 μm and maximum crack extension at the slowest rate (0.002 $min^{-1}$) of 0.15 μm.

## 1. Introduction

Most fracture processes can be classified as either ductile or brittle. The distinction between the two is that plastic deformation is necessary for the spreading of the crack in ductile fracture, while it is not necessary, although it may occur, during spreading of the crack in brittle failure. The size of pre-existing flaws is, therefore, the most important determinant of the fracture stress in brittle fracture. The relationship between fracture stress and flaw size was first stated by Griffith [1] and was found also to depend on the material parameters modulus of elasticity and surface energy. The same process has been considered by Irwin [2] and by Orowan [3, 4], who showed that plastic deformation could accompany brittle failure. In the latter case, Orowan proposed that plastic flow alters the fracture stress but does not contribute to the spreading of the crack; thus the failure mechanism would still be brittle.

Under some conditions, materials susceptible to brittle failure also exhibit delayed failure or static fatigue. This effect has been most prominent in the case of glass. Hillig and Charles [5] have considered this case extensively and have formulated a theory of stress corrosion which has proved successful in explaining the universal fatigue curve of Mould and Southwick [6, 7] obtained with glass. Static fatigue effects in crystalline solids such as aluminium oxide have also been observed. Charles and Shaw [8] have investigated the static and dynamic mechanical properties of 60° sapphire rods and of Lucalox† in wet and dry environments between − 196 and + 850°C. These results showed that the fracture stress was related to the environment and that it was highest in a dry environment. Delayed failure in moist environments was noted and a fatigue limit stress of 0.25 $\sigma_{(-196°C)}$ was determined at 200°C.

Additional evidence of the nature of stress corrosion or static fatigue in sapphire has recently been found by Wiederhorn [9]. The latter

*Present address: Australian Atomic Energy Commision, Research Establishment, Lucas Heights, Sutherland, NSW Australia.
†General Electric Co (of America) trade name for polycrystalline, translucent alumina.

measured the stress and moisture dependence of crack propagation in sapphire, using a technique successfully developed for glass [10, 11], and concluded that the observed dependencies were consistent with the Hillig-Charles mechanism. In both this study and that of Charles and Shaw, the experimental fit to the theory of Hillig and Charles is not so precise as the fit of similar data for glass.

Besides the effect of stress corrosion on the fracture stress of aluminium oxide, arguments have been presented suggesting that microplasticity, which could also cause delayed failure, can be induced during or prior to fracture by concentrated stresses [12]. These arguments arose from an attempt to determine the surface energy by measurements of the stress to extend artificially created cracks. The results gave values of surface energy considered to be approximately ten times the expected values. Further, the data showed that the fracture energy (and fracture stress) increased between + 20 and − 196°C by an amount, independent of static fatigue effects, which could not be explained by variation of elastic or surface free energy parameters with temperature. Thus, these authors concluded that plastic flow entered the fracture process.

More recently, Congleton *et al* [13] have measured the variation with temperature of the fracture energy in polycrystalline aluminium oxide. The fracture energy declined sharply between − 196 and + 250°C and increased even more sharply between 250 and 500°C. In this case, the authors argued that a *necessary* contribution of plastic flow would produce such a minimum if plastic flow also *accompanied* crack propagation so as to produce an increasing plastic work term with increasing temperature. Their conclusion was, therefore, that plastic flow was actually necessary for the fracture process.

Both static fatigue effects* and plastic flow effects in the fracture of aluminium oxide would manifest similar characteristics. In particular, both should give rise to a strain-rate effect on the fracture strength such that the latter would increase with strain-rate. It is important to distinguish between the two causes, however, since each is deleterious to a structural material but would be obviated differently. From the evidence now existing, it seems beyond doubt that static fatigue exists in aluminium oxide. However, the data and arguments of Congleton and co-workers [12, 13] also indicate that plastic flow is involved in the fracture process at room temperature. Thus, it is of interest to show whether or not *de facto* static fatigue can occur in sapphire irrespective of the environment.

## 2. Experimental method

The sapphire filament used in this investigation was grown from the melt using a technique described elsewhere [14]. Details of the structure and usual mechanical properties of this filament have also been published [15-17]. With the exception of treatments specifically described below, all filament used was in the as-grown condition. The filament is grown in an argon atmosphere and is coated with paraffin or epoxy resin containing a silane before leaving the furnace atmosphere. This procedure is normally carried out to avoid damaging the filament by abrasion during handling; we will claim this mechanical protection as a factor in the validity of our conclusions. All of the filament had the axial orientation parallel to [0001] and was 0.20 to 0.23 mm diameter. All of the testing was carried out with samples from three individual lengths of filament. Each length was long enough so that complete experiments could be conducted with samples taken from a single long filament. Starting properties of the three lengths are summarized in Table I.

TABLE I As-grown condition of three lengths of sapphire filament. Strengths determined at $\dot{\epsilon} = 5 \times 10^{-3}$ min$^{-1}$

| Filament | Growth speed (cm min$^{-1}$) | Tensile strength (kg mm$^{-2}$) | Coating |
|---|---|---|---|
| A | 3.8 | 232 | Epoxy |
| B | 4.4 | 268 | Paraffin |
| C | 4.4 | 292 | Epoxy |

Tensile tests were carried out at various strain-rates using samples having a 2.5 cm gauge length. Samples were gripped by cementing with epoxy into corrugated cardboard tabs, as described previously [18]. Testing was carried out with a constant cross head velocity testing machine. Deflection was not measured and load versus time was recorded on the *x-y* recorder supplied with the machine. At high strain-rate (2.0 min$^{-1}$), the response time of the recorder was not short

*Static fatigue is nearly always understood to refer to environmental causes of premature failure.

enough to record the peak load. Thus, at this strain-rate, the load was recorded by photographing an oscilloscope trace made from the output of the bridge circuit taken before rectification. The output was carefully calibrated using dead weights.

A study to determine the origin of fracture was also carried out. Failed samples often shatter completely and usually shatter near the fracture origin. Samples were encased in epoxy and fractured in tension in order to determine if the surface examined was the actual fracture surface. These fracture surfaces were examined both by optical and scanning electron microscopy.

## 3. Structure, microstructure, and fracture origin

The samples used in this investigation were characterized by X-ray diffraction and optical microscopy. The sample axis was parallel to [0001] within approximately 1°. Optical studies of the microstructure were also carried out as described elsewhere [16]. A typical view of the longitudinal midplane (parallel to and coinciding with the axis) is presented in Fig. 1. The features of this micrograph which are pertinent and typical are the dispersion of $\sim$ 1 μm diameter voids and the void-free shell of 20% of the filament radius at the surface. Also, by and large, the voids are situated on rhombohedral planes ($\{\bar{1}012\}$ with $c/a = 2.73$). These planes are the only reported slip and twin planes for the present orientation which could have a non-zero component of resolved shear stress under axial tension [19]. The preferred arrangement of voids on this plane is such that relatively large areas of the slip system would see both applied and concentrated resolved shear stresses. In addition, since voids lie on a series of closely spaced and parallel slip planes, the capability of slip band formation, at least over small volumes of material, exists.

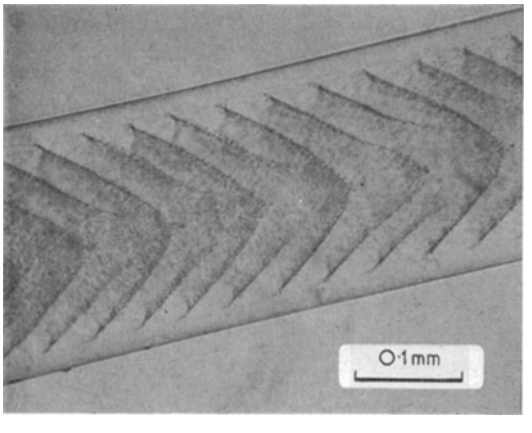


*Figure 1* A typical transmission photomicrograph of the longitudinal midplane of the sapphire filament (parallel to and coinciding with the axis). The microvoids lie mainly on rhombohedral planes except near the surface, which is void-free to a depth of about 25 μm.

The fracture surfaces of samples embedded in epoxy prior to testing are typified by the micrograph in Fig. 2. It is comprised of cleavage surfaces with river markings which converge to a single point. The point of convergence is not at the filament surface, but is located within the sample near the junction of the void-free shell and the voided region. These observations are qualitatively similar to those reported earlier by LaBelle and Hurley [20] in filamentary material. Internal fracture origin has also been reported by Mallinder and Proctor [21] who examined the fracture surfaces of flame-polished sapphire rods ruptured in pure bending. They noted that samples fracturing at the highest strengths often did so from internal defects of the type found in the Verneuil rods tested. LaBelle and Hurley [20] also noted that with degraded filament exhibiting low fracture strengths ($\sim$ 200 kg mm$^{-2}$) fracture origin was clearly located at the filament surface.

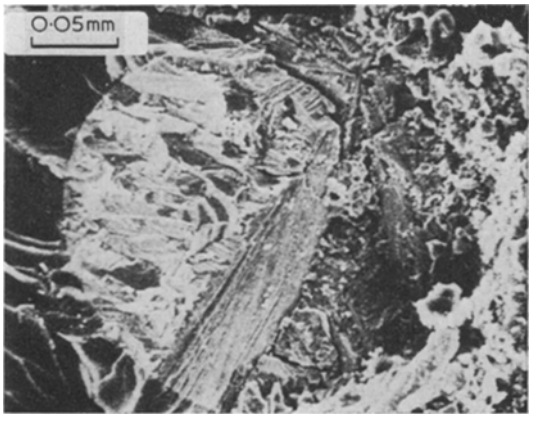


*Figure 2* Scanning electron micrograph of filament surface after fracturing in tension. River markings are found to converge to a point within the sample near the junction of the void-free shell and the voided internal region (see Fig. 1).

## 4. Strain-rate dependence of the fracture stress

Filament lengths A and B (Table I) were used in the as-grown condition to measure the variation in fracture stress with strain-rate. To negate any systematic variation in filament strength within each length, the samples were drawn alternately in four groups until there were seven samples in each group for filament A and ten for filament B. The data for filament A extend only to a strain-rate of 0.2 $min^{-1}$.

The variation in fracture stress for both filament A and B with strain-rate is tabulated in Table II and is also plotted in Fig. 3. The effect was substantial with fracture stress increasing 18% over 2 orders of magnitude strain-rate increase for filament A, and 30% over 3 orders of magnitude strain-rate increase for filament B.

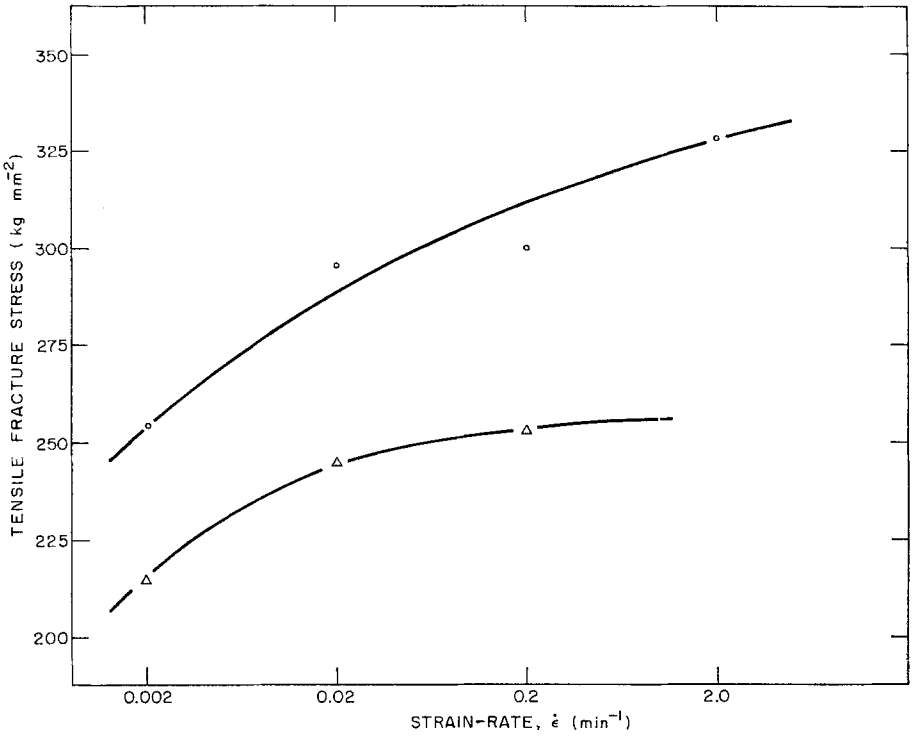


*Figure 3* Tensile fracture stress versus strain-rate. Δ, filament length *A* (each point is average of seven tests); o, filament length *B* (each point is average of ten tests).

TABLE II Strain-rate and fracture stress data for filament lengths A and B.

| | Number of samples tested | Strain-rate ($min^{-1}$) | Average fracture stress (kg $mm^{-2}$) | s.d.* of fracture stress (kg $mm^{-2}$) |
|---|---|---|---|---|
| Filament A | 7 | 0.002 | 215 | 10 |
| | 7 | 0.020 | 245 | 20 |
| | 7 | 0.200 | 253 | 22 |
| Filament B | 10 | 0.002 | 254 | 35 |
| | 10 | 0.020 | 296 | 51 |
| | 10 | 0.200 | 300 | 34 |
| | 10 | 2.000 | 328 | 65 |

*Standard deviation.

Two-sided *t*-tests were carried out using the means and standard deviations listed in Table II and a significance level of 0.975. These showed that the changes in tensile strength were not the result of statistical fluctuations.

A second group of experiments was carried out to (1) show whether or not static fatigue could be used to explain this strain-rate dependence, and (2) determine the prerequisites for static fatigue in this material. Samples taken from filament C were tested at 0.002 $min^{-1}$, the slowest strain used in the previous tests, under a variety of conditions. As indicated in Table I, this filament was coated with epoxy immediately after growth. The results of these tests under five different conditions (C1, C2, C3, etc.) are shown in Fig. 4. The sample groups C1, C2 and C3 demonstrate the effect of water at fixed strain-rate on both coated and uncoated samples. The standard deviation within each group of eight samples was about 5% with the maximum variation between groups only 2.5%. Thus, varying the humidity during testing of coated or uncoated samples from 40% to water immersion did *not* affect the fracture strength. In contrast, the groups of samples C4 and C5 show the effect of moisture when the sample surfaces are uncoated and deliberately damaged. The strength fell 33%, to 195 kg $mm^{-2}$, as a result of deliberate surface degradation. It further declined by 26% of this lower value to 140 kg $mm^{-2}$ on immersion in water. This result clearly shows that the introduction of surface flaws leads to moisture sensitive fracture behaviour. Therefore, taken together, these results show that *as-grown* filament, whether coated or uncoated, does not exhibit moisture dependent fracture strength at a tensile strain-rate of $2 \times 10^{-3}$ $min^{-1}$. In view of the internal fracture origin in as-grown filament, as evidenced by the SEM study, this conclusion is not entirely unexpected. On the other hand, uncoated and deliberately damaged filament shows a large loss of strength and, in addition, shows a further large strength decrease on water immersion when tested with a tensile strain-rate of $2 \times 10^{-3}$ $min^{-1}$.

Thus, under conditions in which fracture proceeds by propagation of surface flaws, the fracture stress is moisture sensitive, and strain-rate sensitivity here would be attributable to

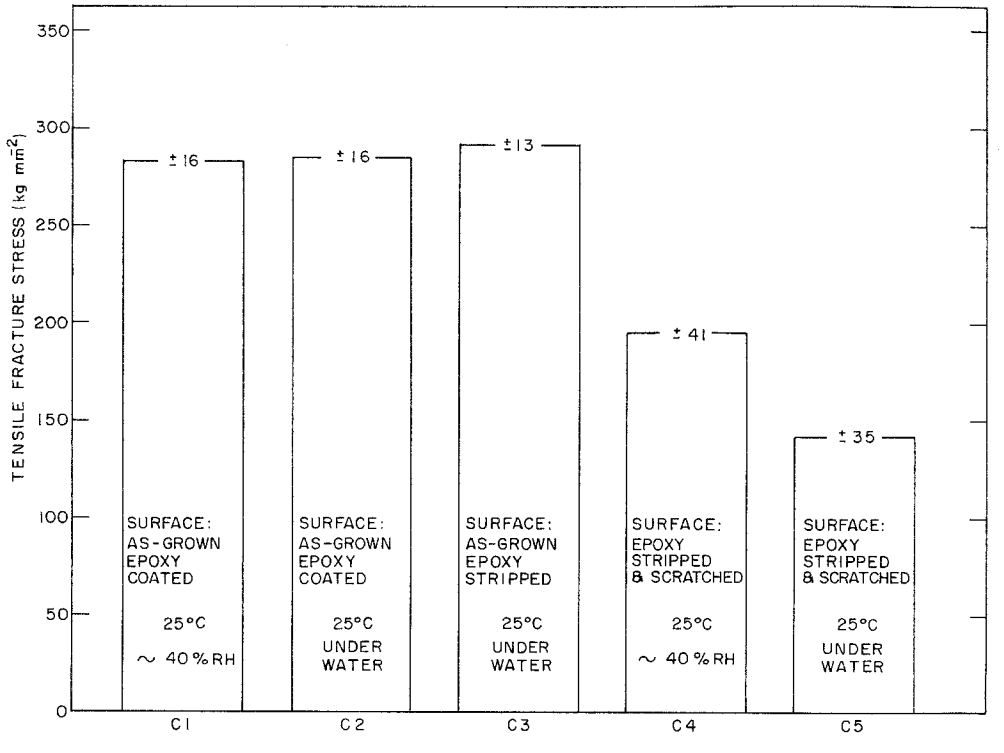


*Figure 4* Bar graph showing the effect of surface condition and test environmental humidity on the tensile fracture stress of samples from filament C.

static fatigue. However, when the surface is coated and is in the as-grown condition (damage-free), the fracture stress is not sensitive to moisture; yet, as shown in Fig. 3, it exhibits a strain-rate dependence.

## 5. Proposed mechanism of fracture nucleation

Plastic deformation can contribute to the fracture process in both ductile and brittle fractures. In the latter, the plastic deformation is incidental to the fracture itself; thus, while the fracture stress may be affected, this effect would be *during* rather than *after* initiation of crack propagation. The flow stress of sapphire at elevated temperature is known to be strain-rate sensitive giving the result that increasing strain-rate increases the flow stress [22, 23]. This sensitivity is observed for both the yield stress and the flow stress. Since there is no reason not to expect a similar effect in the realm of micro-plasticity, then its effect on fracture phenomena should decrease with increasing strain-rate. If plastic flow along the advancing crack represents its only contribution to fracture, then the fracture stress should approach a constant, lower value as the strain-rate increases. This is opposite to the effect noted in the present instance. If, on the other hand, plastic flow precedes fracture and alters the fracture stress, then it could either aid fracture by crack nucleation or crack extension prior to crack propagation (decrease the fracture stress) or impede fracture (increase the fracture stress) by plastic blunting. The latter would not be expected on the basis of the number of available slip systems [13], and would anyhow affect the fracture stress in the opposite sense to that observed. However, any flow-induced nucleation or crack-extension mechanisms would produce a direct dependence of fracture stress on strain-rate, as observed in the present case. This follows from the strain-rate dependence of the flow stress, since, as the amount of flow decreases, the fracture must proceed by propagation of smaller and smaller flaws.

In the present case, crack extension rather than nucleation would be expected, since large numbers of small flaws (voids) are present in the microstructure. Based on the observed dependence of fracture stress on strain-rate and on the availability of suitably oriented small flaws, we propose a mechanism for pre-failure crack growth founded upon a model formulated by Orowan [24]. The same mechanism has been proposed [25] for the dependence of fracture stress in 60° sapphire crystals on strain at temperatures between 1100 and 1500° C. In the latter case, the crystals were observed to display plastic behaviour by slip on the basal system.

The mechanism for crack growth proposed by Orowan was originally suggested to describe fracture in MgO, NaCl, KCl and similar crystals for which plastic flow is established. The model is shown in Fig. 5. Slip occurs on a set of planes at some angle to the tensile axis. A flaw at B produces a concentrated tensile stress at its tip which is less than the critical stress for propagation. If a dislocation passes near B, its stress

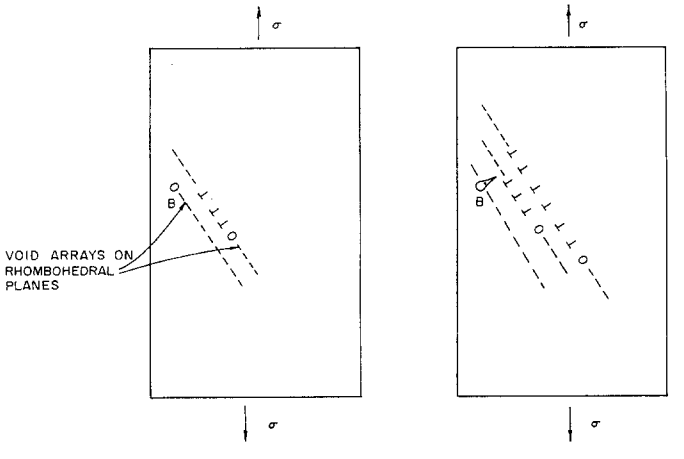


*Figure 5* Schematic representation of sub-critical crack growth under applied tensile load. Dislocations generated by the stress concentration of voids on adjacent rhombohedral planes interact with the stress field of the void at B to produce crack lengthening (Based on Orowan's (1959) Model).

field interacts with that of the crack and the combined stress field may be great enough to produce crack extension. This incremental extention relieves part of the stress, however, and growth is halted, provided that the critical stress for the larger crack is still not exceeded by the applied stress. The rate of growth of the crack to its critical length may then be visualized as proceeding at the same rate as the increase in slip-band width. Stofel and Conrad [25] treated the fracture stress dependence on total strain above 1100°C in this way and showed their data to be consistent with a linear rate of slip-band growth. In addition, their data suggested a saturation effect which they interpreted as impingement of the slip-bands.

In the absence of direct observation, the most important points which should be proved to establish the feasibility of such a mechanism of subcritical crack growth in sapphire at room temperature are the attainment of the flow stress as the fracture stress is approached, the proper relationship between strain-rate and fracture stress (as argued above), and the elimination of other causes (static fatigue) which could give the same effect. The latter two conditions are satisfied by the present work. The occurrence of plastic flow at room temperature in tensile tests of sapphire has not been proved directly. However, arguments for pre-fracture plasticity have been presented in the literature [12, 13], In the case of the present fibres, it has been shown that microscopic voids exist in the material and that these flaws could act as stress concentrators to increase the stress near the expected flow stress of sapphire in a tensile test [20]. Further, the description of the microstructure given in Section 3 shows that these flaws exist in such abundance and relative proximity that local plastic flow giving small slip-bands passing close to other flaws becomes a reasonable assumption. Finally, Rice [26] has shown the yield stress deduced from microhardness to be the upper limit for compressive fracture strength in $Al_2O_3$.

We have examined the flaw size ($c_0$) and amount of flaw growth that would be necessary to cause fracture at the present levels, following an analysis similar to that used by Stofel and Conrad [25]. Slip-bands are assumed to have a width $w$ (parallel to the crack) and rate of growth $w' = dw/dt$. The time during which the load is applied is given by $\Delta t = \epsilon_f/\dot{\epsilon}$, where $\epsilon_f$ is the strain at failure. Slip-band growth can occur only during part of this time since its growth is assumed not to occur before the yield stress is reached. Thus the crack length at failure may be taken as $c = c_0 + fw'\,\Delta t$, where $f$ is the fraction of $\Delta t$ during which the yield stress is exceeded. Inserting this value in the Griffith-Orowan equation gives:

$$\sigma_f^2 = \frac{EP}{2(c_0 + fw'\,\Delta t)} \qquad (1)$$

where $E$ is the Young's modulus and $P$ is the work of fracture. This expression can be rearranged giving

$$\frac{EP}{2} \times \frac{1}{\sigma_f^2} = fw'\,\Delta t + c_0 \cdot$$

Using values of $E = 46.4 \times 10^{11}$ dyn cm$^{-2}$ and $P = 10^4$ erg cm$^{-2}$, $EP/2\sigma_f^2$ is shown plotted versus $\Delta t$, for two sets of data (from Table II), in Figs. 6 and 7. The extrapolation of these curves through the vertical axis at $\Delta t = 0$ gives $c_0$ values which range from 0.22 to 0.26 μm for the stronger material (Fig. 7) to 0.37 to 0.39 μm for the weaker material (Fig. 6). The largest increase in crack length is at the slowest strain-rate and is approximately 0.15 μm.

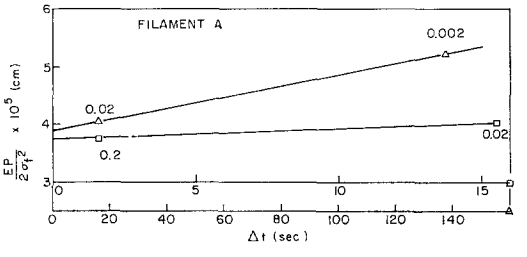


*Figure 6* $EP/2\sigma_f^2$ plotted versus time available for flaw growth to critical size, using the data for filament A tabulated in Table II.

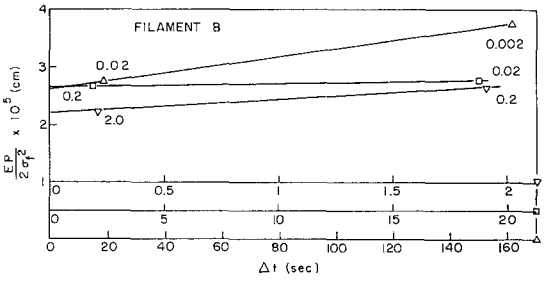


*Figure 7* $EP/2\sigma_f^2$ plotted versus time available for flaw growth to critical size $\Delta t$, using the data for filament B tabulated in Table II.

## 6. Conclusions

As-grown, single crystal sapphire filaments with *c*-axis orientation have tensile fracture strengths at a strain-rate of 0.002 $min^{-1}$ which are independent of the amount of water in the testing environment. However, the introduction of surface flaws by deliberate scatching causes a reduction in strength which was dependent on the test environment moisture content. These correlations were confirmed by SEM evidence of internal fracture origin in as-grown material.

Samples in the as-grown condition fail at strength levels dependent on strain-rate, such that an increase in strain-rate from 0.002 to 2.0 $min^{-1}$ caused the fracture strength to increase by 30% of the lowest average value. It is proposed that this latter behaviour is not caused by static fatigue and is consistent with the Orowan model of subcritical crack extension in brittle materials. Background flaw sizes in the range 0.22 to 0.39 μm and maximum crack extension at the slowest strain-rate (0.002 $min^{-1}$) of 0.15 μm have been calculated using experimental data.

## Acknowledgements

The authors gratefully acknowledge the experimental assistance of J. Bailey. This work was sponsored by the Air Force Materials Laboratory, Non-Metallic Division, Wright-Patterson Air Force Base, Ohio.

## References

1. A. A. GRIFFITH, *Trans. Roy. Soc.* **A221** (1921) 163.
2. G. R. IRWIN, "Fracturing of Metals" (*A.S.M.*, Cleveland, Ohio, 1948) p. 147.
3. E. OROWAN, *Rep. Prog. Phys.* **12** (1949) 185.
4. *Idem, Weld. J.* **34** (1955) 157
5. W. B. HILLIG and R. J. CHARLES, "High Strength Materials" (Ed. V. H. Zackay) (Wiley, New York, 1965) p. 682.
6. R. E. MOULD and R. D. SOUTHWICK, *J. Amer. Ceram. Soc.* **42** (1959) 542.
7. *Idem, ibid* **42** (1959) 582.
8. R. J. CHARLES and R. R. SHAW, General Electric Laboratory Report No. 62-RL-3081M (1962), General Electric Co. of America.
9. S. M. WIEDERHORN, *Inter. J. Fracture Mech.* **4** (1968) 171.
10. *Idem*, "Environmental Sensitive Mechanical Behavior of Materials" (Eds. A. R. C. Westwood and N. S. Stoloff) (Gordon and Breach, New York, 1966).
11. S. M. WIEDERHORN, *J. Amer. Ceram. Soc.* **50** (1967) 407.
12. J. CONGLETON and N. J. PETCH, *Acta. Metallurgica* **14** (1966) 1179.
13. J. CONGLETON, N. J. PETCH, and S. A. SHIELS, *Phil. Mag.* **19** (1969) 1795.
14. H. E. LABELLE, *Mat. Res. Bull.* **6** (1971) 571.
15. G. F. HURLEY and J. T. A. POLLOCK, *Met. Trans.* **3** (1972) 397.
16. J. T. A. POLLOCK, *J. Mater. Sci.* **7** (1972) 631.
17. *Idem, ibid* **7** (1972) 649.
18. G. F. HURLEY, *ibid* **7** (1972) 471.
19. A. H. HEUER, *Proc. Brit. Ceram. Soc.* **15** (1970) 173.
20. H. E. LABELLE and G. F. HURLEY, *S.A.M.P.E. Journal* **6** (1970) 17.
21. F. C. MALLINDER and B. A. PROCTOR, *Phil. Mag.* **13** (1966) 197.
22. M. L. KRONBERG, *J. Amer. Ceram. Soc.* **45** (1962) 274.
23. H. CONRAD, G. STONE, and K. JANOWSKI, *Trans. Met. Soc. AIME* **233** (1965) 889.
24. E. OROWAN, "Fracture" (Eds. B. L. Averbach, D. K. Felbeck, G. T. Hahn and D. A. Thomas (MIT Press, Cambridge, Mass., 1959) p. 225.
25. E. STOFEL and H. CONRAD, *Trans. Met. Soc. AIME* **227** (1963) 1053.
26. R. W. RICE, "Proc. of the Symposium of Ceramics in Severe Environments" (Eds. W. W. Kriegel and H. Palmour III) (Plenum Press, New York, 1971) p. 195.

Received 10 April and accepted 15 May 1973.